| | |
|---|---|
| **Título artículo / Títol article:** | **Toward an understanding of the hydrogenation reaction of $MO_2$ gas-phase clusters (M = Ti, Zr, and Hf)** |
| **Autores / Autors** | **González Navarrete, Patricio; Calatayud Antonino, Mónica; Andrés Bort, Juan; Ruipérez, F.; Roca Sanjuan, Daniel** |
| **Revista:** | **Journal of Physical Chemistry A** |
| **Versión / Versió:** | **Post-print** |
| **Cita bibliográfica / Cita bibliogràfica (ISO 690):** | **GONZALEZ-NAVARRETE, Patricio, et al. Toward an Understanding of the Hydrogenation Reaction of MO2 Gas-Phase Clusters (M= Ti, Zr, and Hf). The Journal of Physical Chemistry A, 2013, vol. 117, no 25, p. 5354-5364.** |
| **url Repositori UJI:** | http://hdl.handle.net/10234/85029 |

# Toward an Understanding of the Hydrogenation Reaction of $MO_2$ Gas Phase Clusters (M = Ti, Zr and Hf)

P. González-Navarrete*[1,2,3], M. Calatayud[2,3,4] J. Andrés[1], F. Ruipérez[5] and D. Roca-Sanjuán[6]

[1]Departament de Química Física i Analítica, Universitat Jaume I, 12071 Castelló, Spain

[2] UPMC Univ Paris 06, UMR 7616, Laboratoire de Chimie Théorique, F-75005, Paris, France

[3] CNRS, UMR 7616, Laboratoire de Chimie Théorique, F-75005, Paris, France.

[4] Institut Universitaire de France

[5] Kimika Fakultatea, Euskal Herriko Unibertsitatea (UPV/EHU) and Donostia International Physics Center (DIPC), P.K. 1072, 20080 Donostia, Euskadi, Spain

[6] Instituto de Ciencia Molecular, Universitat de València, P. O. Box 22085, ES-46071 València, Spain

Corresponding author: pgonzale@qfa.uji.es

**Abstract**

A theoretical investigation using density functional theory (DFT) has been carried out in order to understand the molecular mechanism of dihydrogen activation by means of transition metal dioxides $MO_2$ (M = Ti, Zr and Hf), according to the following reaction: $MO_2 + H_2 \rightarrow MO + H_2O$. B3LYP/6-311++G(2df,2pd)/SDD methodology was employed considering two possible reaction pathways. As first step the hydrogen activation by M=O bonds yields to metal-oxo hydride intermediates O=MH(OH). This process is spontaneous for all metal dioxides, and the stability of the O=MH(OH) species depends on the transition metal center. Subsequently, the reaction mechanism splits into two paths; the first one takes place passing through the $M(OH)_2$ intermediates yielding to products whereas the second one corresponds to the direct formation of the product complex $OM(H_2O)$. A two state reactivity mechanism was found for $TiO_2$ system whereas for $ZrO_2$ and $HfO_2$ no spin-crossing processes were observed. This is confirmed by CASSCF/CASPT2 calculations for $ZrO_2$ that lead to the correct ordering of electronic states not found by DFT. The results obtained in the present paper for $MO_2$ molecules are consistent with the observed reactivity on surfaces.

**Key words**: metal oxides, $TiO_2$, $ZrO_2$, $HfO_2$, hydrogenation reaction, DFT calculations, spin crossing.

## 1. Introduction

Transition metal oxides are important in chemistry due to their ability to catalyze numerous oxidation reactions as well as their use as support materials[1-4] for different commercially relevant reactions.[5, 6] Likewise, the utilization of simple metal oxides clusters has served as interesting models in understanding the nature of active species in catalysis at molecular level.[7] In particular, the activation of $H_2$ by metal centers is a fundamental step in nearly all metal catalytic hydrogenation reactions.[8-10] The reactions of molecules involving transition metal oxides and $H_2$ provide well-defined molecular models pertinent to mechanistic understandings of the dihydrogen in some catalytic and biochemical processes.[11] Gas-phase and theoretical studies can be used as a helpful tool to gain complementary insights into the molecular mechanism and intrinsic reactivity, as well as to provide an ideal field for detailed experiments of the energetic and kinetics of any bond-making and bond-breaking process at molecular level.[12] In this sense, the theoretical works can provide a deeper insight into the principles governing the reactions of transition metal oxides.

Due to their enormous applications as catalytic materials, the group IV metal oxides have been widely studied both experimentally and theoretically.[13] For example, $TiO_2$ is one of the most technologically important oxide materials widely studied as a prototypical transition metal oxide because of its rather simple electronic structure.[14-16] Thanks to its photocatalytic properties, $TiO_2$ has been utilized in the production of hydrogen gas by photoelectrolysis of water[17, 18] and conversion of $CO_2$ in aqueous medium to methanol.[19] Although considered less important than $TiO_2$ for catalysis, $ZrO_2$, $HfO_2$, and materials using these oxides are also known for their catalytic activities. For instance, $ZrO_2$ is a well known solid acid-catalyst[20] and as a result, the mixture of $TiO_2$-$ZrO_2$ oxides has excellent catalytic properties showing interesting acid-base

surface properties, high surface area, great thermal stability and strong mechanical strength.[21] Additionally, $HfO_2$ has recently been used to replace the $SiO_2$ gate dielectric due to its high dielectric constant in order to further miniaturize microelectronic components in metal oxides semiconductors.[22, 23] $TiO_2$, $ZrO_2$, and $HfO_2$ oxides have also been utilized to catalyze the aromatization of $C_{6+}$ alkanes.[20]

While chemical reactions of the bare transition metal oxide cations with $H_2$ have received a significant interest,[24-37] neutral metal oxides have gained much less attention.[38-50] Recently Zhou et al.[51] have reported a combined experimental and theoretical study on the hydrogenation reactions by group V metal dioxides using matrix isolation spectroscopy. These results show a thermodynamically favorable reaction for the dihydrogen cleavage process with small barrier for $VO_2$, whereas $NbO_2$ and $TaO_2$ dioxide molecules react with dihydrogen to give primarily $NbO_2(\eta^2\text{-}H_2)_2$ and $TaO_2(\eta^2\text{-}H_2)_2$ complexes and subsequently O=NbH(OH) and O=TaH(OH) molecules, respectively, via photoisomerization in combination with $H_2$ elimination under UV-visible light excitation.

In this work, we present a theoretical study on the reaction mechanism for the dihydrogen activation by neutral group IV metal dioxides ($MO_2$, M = Ti, Zr, and Hf) according to the following reaction:

$$MO_2 + H_2 \rightarrow MO + H_2O \quad (1)$$

The first step is the favorable formation of $MO_2(H_2)$ adduct. Then, a cleavage process of $H_2$ takes place involving M=O bonds to yield a metal-oxo hydride intermediate O=MH(OH). Subsequently, two possibilities have been explored: i) a two-step mechanism passing through $M(OH)_2$ intermediates, and then a proton migration yielding the final complex $MO(H_2O)$ (Path 1) or ii) direct formation of products by means of proton transfer from metal atom toward the hydroxyl group to render the

product complex $MO(H_2O)$ (Path 2; see scheme 1). The whole process involves the reduction of the transition metal from a formal oxidation state of M from (IV) to (II), and, depending on the metal center, a spin-crossing process along the reaction pathway might control the chemical reactivity. The effects of the transition metal size as well as their specific reactivities are analyzed.

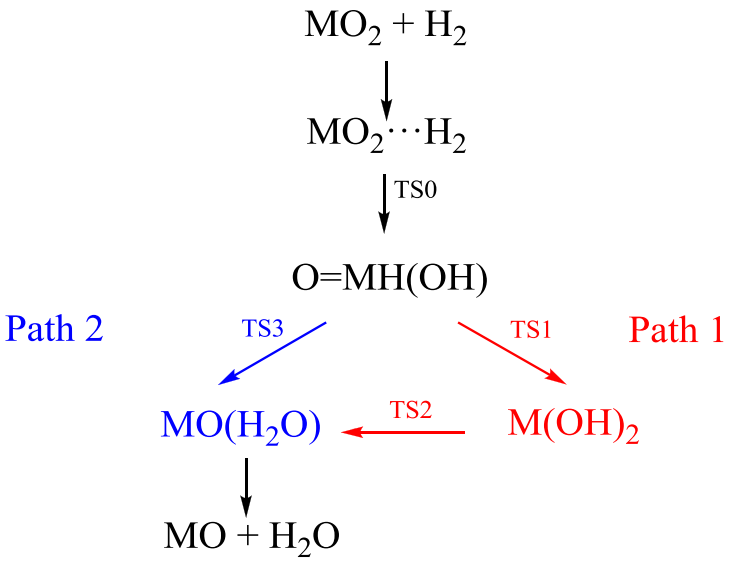


**Scheme 1**

The paper is structured in four sections: First, the computational methods are described. Next, the results are presented in two subsections, focusing primarily on the validation of computing method and on the chemical reactivity (activation of dihydrogen and competition between the alternative mechanisms). The next section is devoted to the discussion of the results. Finally, the conclusions of the work are given.

## 2. Computational Methods

Density functional theory (DFT) calculations have been performed using the Gaussian03 code.[52] The geometries of the reactants, products, intermediates, and transition states have been optimized using the hybrid DFT, using Becke's three-parameter nonlocal exchange functional with the nonlocal correlation functional of Lee–Yang–Parr (B3LYP).[53, 54] A frequency analysis has been carried out to determine the nature of the optimized structures as minima or transition states. Connections of the transition states (TSs) between two local minima have been confirmed by intrinsic reaction coordinate calculations.[55] The 6-311++G(2df,2pd) basis set has been used for the H and O atoms, whereas for transition metal atoms (M = Ti, Zr, and Hf) the Stuttgart pseudopotential[56] (labelled as SDD in Gaussian 03) has been utilized.

In order to compare with more accurate ab initio calculations multiconfigurational second-order perturbation theory (CASSCF/CASPT2)[57] energy computations have been carried out for Zr mechanisms to describe the correct ordering of the singlet and triplet states. The triple-ζbasis set of all-electron atomic natural orbital (ANO-RCC)[58] type with the primitive set Zr(21s18p13d6f4g2h)/O(14s9p4d3f2g)/H(8s4p3d1f) contracted to Zr[7s6p4d2f1g]/O[4s3p2d1f]/H[3s2p1d] was used throughout. The active space comprises the 4d and 5s shells of Zr, the 2p shell of O, and the 1s shell of H. It represents a total of 14 electrons distributed among 14 molecular orbitals. One root was used in the CASSCF/CASPT2 computations of the singlet and triplet states with no symmetry constraints. The ionization potential electron affinity (IPEA)-corrected zeroth-order Hamiltonian with the default value of 0.25 au was employed.[59] The 4s and 4p orbitals of Zr and the 2s orbital of O are also correlated dynamically in the CASPT2 computations. In order to minimize weakly interacting intruder states, the imaginary level-shift technique with a parameter of 0.2 au was employed.[60] All the

CASSCF/CASPT2 calculations were performed by the MOLCAS-7 package of software.[61]

On the other hand, from a fundamental point of view, the chemical reactivity of transition metal oxides is strongly influenced by the availability of multiple low-lying electronic states in these species.[31, 62, 63] This means that the reactions involve several electronic states that may also have different spins, namely, it should involve spin-conserving and spin-inversion processes.

To classify these reactions which involve participation of more than a single spin surface, the two-state reactivity (TSR) paradigm has been considered.[64, 65] In particular, the rate of chemical rearrangements that involves a change in the spin state can be limited by the transition state (TS) of the process or by the crossing efficiency between the potential energy surfaces (PES). Therefore, it is necessary not only to locate and to characterize the stationary points on each PES (minima and TSs) but also to identify the regions where the relevant spin states lie close in energy (minimum energy crossing point, MECP). Thus, TSR involving transition metals has been acknowledged to play a key role in many reactions ranging from heme enzymes and polyoxometalates[64] to hydrocarbons with vanadium oxides.[66] Minimum energy crossing points MECPs have been localized and characterized by means of the mathematical algorithm developed by Harvey and coworkers.[67]

## 3. Results

a) Validation of the computational method

In order to check the validity of the computing method, geometries and vibrational frequencies have been calculated for $MO_2$ and MO molecules. The results have been analyzed and compared with previous experimental data. At the ground electronic states ($^1A_1$), the most stable structures of $TiO_2$, $ZrO_2$, and $HfO_2$ are closed shell with $C_{2v}$ symmetry. The calculated bond lengths M-O, bond angles <OMO and harmonic vibration frequencies for $MO_2$ molecules are listed in Table 1, which have been found in good agreement with the experimentally observed values.

**Table 1.** Calculated (at B3LYP/6-311++G(2df,2pd)/SDD level) and observed M-O distances (Å), <OMO angles (deg), and vibrational frequencies ($cm^{-1}$) for transition metal dioxides $MO_2$ $C_{2v}(^1A_1)$[a]

| molecule | M-O | <OMO | $\nu_1$ | $\nu_2$ | $\nu_3$ | M-O[obs], <OMO[obs] | vib freq from matrix IR($cm^{-1}$)[b] |
|---|---|---|---|---|---|---|---|
| $TiO_2$ | 1.639 | 111.5 | 1.003 | 347 | 985 | 111-115[b] | 946.9($\nu_1$), 917.1($\nu_3$) |
| $ZrO_2$ | 1.787 | 107.4 | 918 | 304 | 860 | 1.7710[c], 108.11[c] | 884.3($\nu_1$), 818.0($\nu_3$) |
| $HfO_2$ | 1.799 | 107.4 | 889 | 292 | 820 | 1.7764[d], 107.51[d] | 883.4($\nu_1$), 814.0($\nu_3$) |

[a] $\nu_1$ symmetric stretching, $\nu_2$ bending and $\nu_3$ asymmetrical stretching
[b] Observed values corresponding to $TiO_2$, $ZrO_2$ and $HfO_2$ molecules: Ref. 68
[c] Ref. 70 [d] Ref 69

It is well known that density functional based calculations overestimate the values of vibrational frequencies, especially for stretching modes, however no additional scaling factors have been applied to the calculated frequencies. In particular, for $TiO_2$ and $ZrO_2$ molecules the calculated harmonic B3LYP/6-311++G(2df,2pd)/SDD frequencies for symmetric stretching $\nu_1$ and asymmetric stretching $\nu_3$ bands were overestimated in the range of 56-33 $cm^{-1}$ and 67-42 $cm^{-1}$, respectively[68] (see Table 1). However, $HfO_2$ molecule shows the stretching bands in the region of 889 $cm^{-1}$ (symmetric) and 820 $cm^{-1}$ (asymmetric) which are in excellent agreement with the experimental values of 883 $cm^{-1}$

and 814 $cm^{-1}$, respectively, reported by Lesarri et al.[69] In addition, the calculated frequency for the bending mode of $ZrO_2$ of 304 $cm^{-1}$ agrees well with the 290 $cm^{-1}$ value determined from the inertial defect.[70]

The most stable structures for the MO molecules (TiO($^3\Delta$), ZrO($^1\Sigma^+$), and HfO ($^1\Sigma^+$)) have been localized in their respective ground electronic states. The calculated bond lengths, and harmonic vibration frequencies for the MO molecules are listed in Table 2. The Ti-O bond length was predicted to be 0.008 Å shorter than its experimental value, whereas the Zr-O and Hf-O distances were calculated longer by an amount of 0.023 and 0.027 Å, respectively. The calculated frequencies for the MO molecules have been overestimated in 37.8 and 18 $cm^{-1}$ for TiO and ZrO, respectively,[71-73] while the calculated frequency for HfO was predicted to be red shifted in 20 $cm^{-1}$ (see Table 2). Thus, both calculated M-O distances and vibrational frequencies were found in good agreement with experimental values.

**Table 2**. Calculated (at B3LYP/6-311++G(2df,2pd)/SDD level) and observed M-O distances (Å), and vibrational frequency ($cm^{-1}$) for transition metal monoxides MO.

| molecule | state | M-O | $\nu$ | M-O$^{obs}$ | $\nu^{obs}$($cm^{-1}$) |
|---|---|---|---|---|---|
| TiO | $^3\Delta$ | 1.612 | 1047 | 1.620[a] | 1009.18[b] |
| ZrO | $^1\Sigma^+$ | 1.735 | 988 | 1.712[c] | 970[c] |
| HfO | $^1\Sigma^+$ | 1.750 | 954 | 1.7231[d] | 974.09[d] |

[a]Ref 71, [b]Ref 73, [c]Ref 70, [d]Ref 69

Previous theoretical works describing the electronic structure of group IV $MO_2$ molecules have been reported including advanced *ab initio* methodologies and DFT calculations [7, 15, 41, 46-48, 50, 74-82]. Besides the accurate prediction of advanced *ab initio* calculations, DFT has been able to give good results for geometric parameters and vibrational analysis. Therefore, the calculated values obtained by using the present DFT methodology are consistent with previous experimental and theoretical reported data.

b) Activation of dihydrogen

The reaction profiles are shown in Figure 1. The reaction proceeds via the $MO_2(^1A_1)$ + $H_2(^1\Sigma_g^+)$ channel with the initial formation of $MO_2(H_2)$ adducts without any barrier. These species are thermodynamically favorable for all $MO_2$ molecules. The formation of $MO_2(H_2)$ adducts are predicted to be 10.1, 7.5, and 10.2 kcal/mol more stable regarding the $MO_2(^1A_1)$ + $H_2(^1\Sigma_g^+)$ asymptote for Ti, Zr, and Hf dioxides, respectively. In agreement with previous results, the reactants form side-on $MO_2(H_2)$ complexes[38, 51] with $C_1$ symmetry. The selected geometric parameters are depicted in Figure 2. From the $MO_2(H_2)$ adducts, a proton transfer process towards one oxygen atom of the metal-oxo bonds takes place to yield O=MH(OH) intermediates via TS0. This can be associated with a heterolytic cleavage process of the hydrogen molecule. The energy barriers are calculated to be 6.8, 5.7, and 2.2 kcal/mol for Ti, Zr, and Hf dioxides, respectively. The TS0 transition states correspond to the typical four-center structure and were predicted to be more stable than their respective ground state reactants, in contrast to the group V metal dioxides where in some cases their corresponding transition states require activation energy.[38, 51] Besides, the O=MH(OH) species were predicted to be exothermic by 39.4, 42.8, and 54.0 kcal/mol for Ti, Zr, and Hf dioxides, respectively. Thus, the exothermicity of this reaction step increases in reverse order as the activation barriers of the dihydrogen cleavage.[38] In this sense, the lower activation energy and the higher stability for the formation of the O=HfH(OH) species implies that the overall $HfO_2 + H_2 \rightarrow$ O=HfH(OH) process is strongly favorable in comparison to the related mechanism in the other metals.

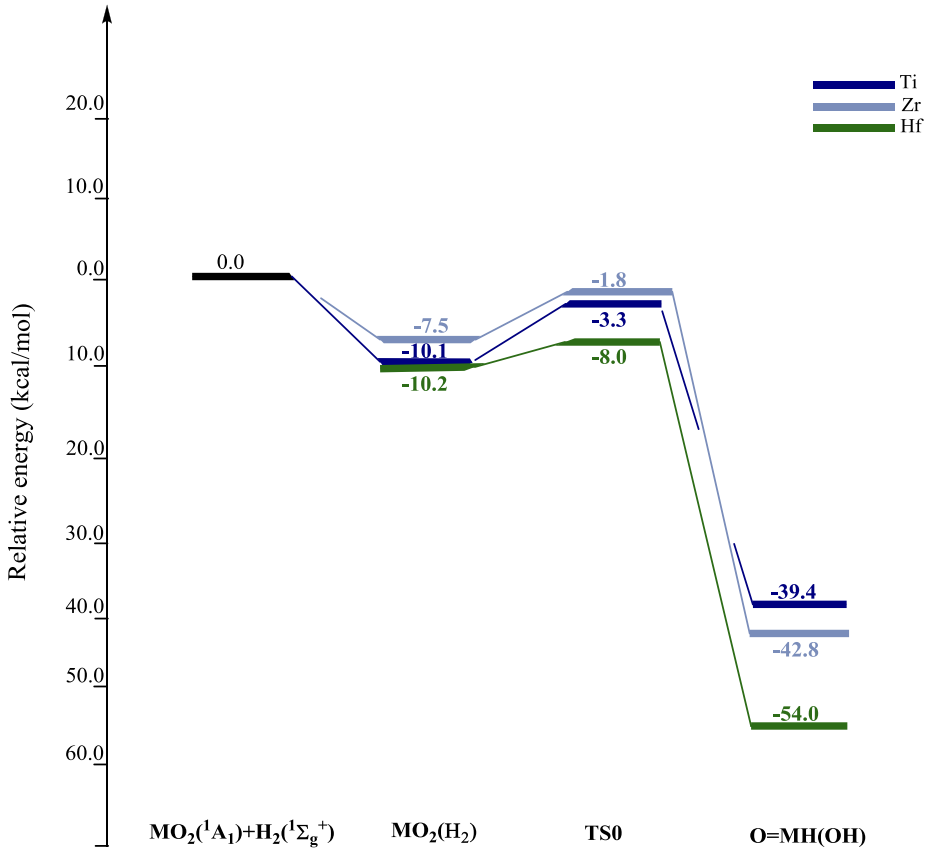


**Figure 1.** Potential energy profiles for the $MO_2$ ($^1A_1$) + $H_2$ → O=MH(OH) step calculated at the B3LYP/6-311++G(2df,2dp)/SDD level of theory.

In a recent study, a spontaneous reaction between $H_2$ and group V metal dioxides has been observed to form O=MH(OH) species.[51] Also, the activation of $H_2$ by tantalum oxides in different oxidation states at cryogenic temperatures has been studied.[38] Their results indicate that the reactivity of tantalum oxides depends on the oxidation state and it increases as follows: $Ta^{V}O_4$>$Ta^{IV}O_2$>$Ta^{II}O$. Our results for group IV metal dioxides show that the activation of $H_2$ and the stability of O=MH(OH) species depends on the metal center, although none experimental evidences have been previously reported in order to support our predictions. In particular, the studied reaction mechanisms concerning the $H_2$ cleavage were found to be exothermic processes yielding to the formation of O=MH(OH) intermediates.

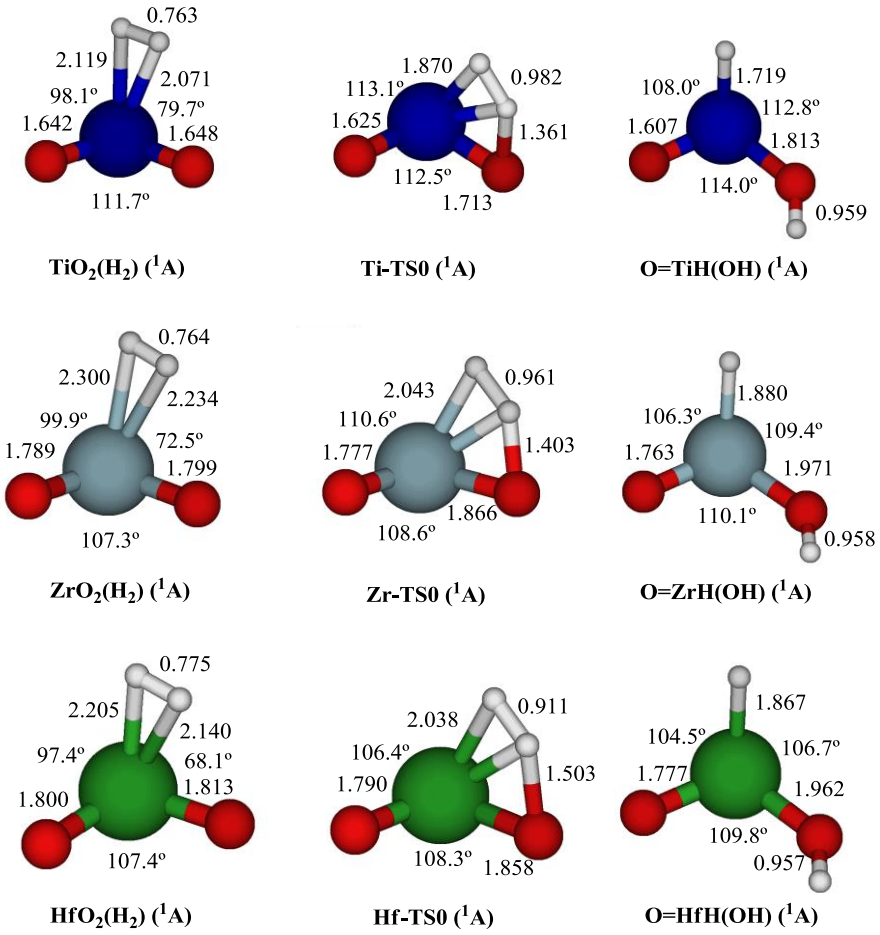


**Figure 2**. Optimized geometric parameters calculated at the B3LYP/6-311++G(2df,2pd)/SDD level of the involved species in the $MO_2(^1A_1)$ + $H_2$ → O=MH(OH) step. Distances in angstroms and angles in degrees.

c) Competition between Path1 and Path2 mechanisms

The formation of products has been considered via two reaction pathways: Path 1 and Path 2. The triplet electronic state has been considered for Ti and Zr dioxides mechanisms while the mechanisms involving Hf only proceed in the singlet electronic state since triplet electronic state has been found considerably higher in energy and therefore it is not considered. In this sense, along the Path1 the formation of products passing through the $M(OH)_2$ species to lead the final product complex $O=M(H_2O)$ is studied, whereas Path 2 corresponds to the direct formation of the $O=M(H_2O)$ products from the O=MH(OH) species. The energy profiles of all studied mechanisms are

depicted in Figure 3. The obtained reaction pathways for each metal oxide are explained as follows:

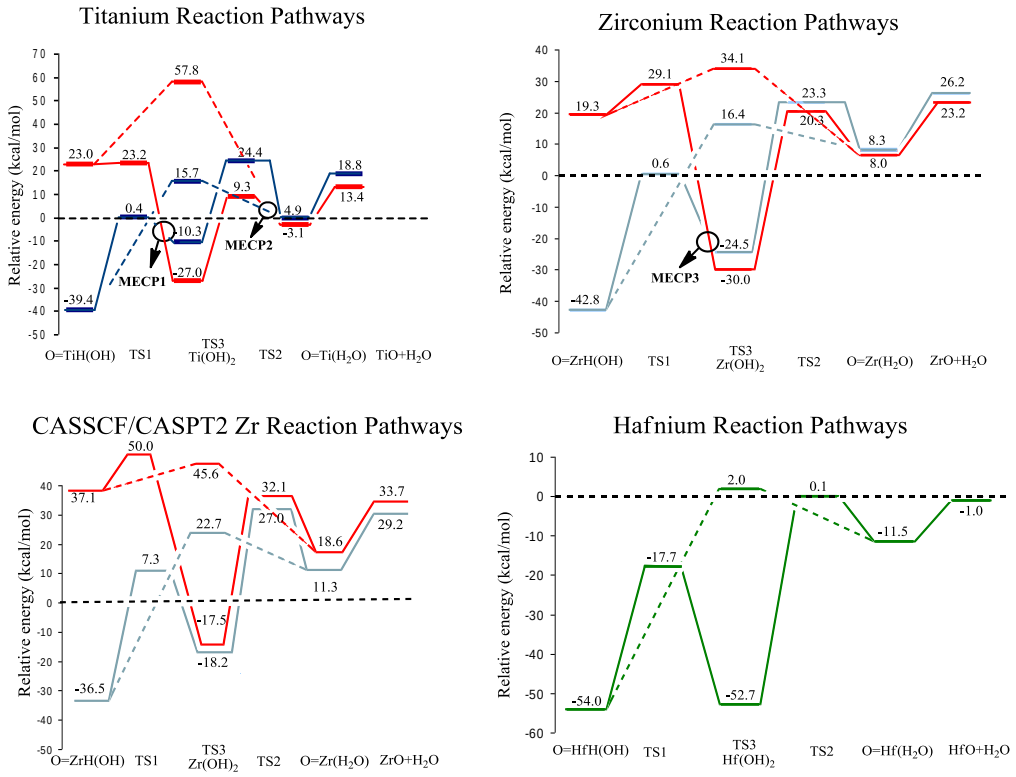


**Figure 3.** Energy profiles for the O=MH(OH) → MO + $H_2O$ step calculated at the B3LYP/6-311++G(2df,2dp)/SDD and CASSCF/CASPT2 level, for Path1 and Path2. Energies (in kcal/mol units) are given relative to the singlet reactants. The plane lines correspond to Path1, whereas the dashed lines correspond to Path2. Red lines correspond to the triplet state, respectively.

**Ti.** The optimized geometric parameters and geometries are depicted in Figure 4. According to Path1, the singlet O=TiH(OH) intermediate transfers one proton from the metal center toward the oxygen atom of the Ti=O bond to yield the $Ti(OH)_2$ intermediate via TS1. The calculated barrier heights of this process are 39.8 and 0.2 kcal/mol for singlet and triplet, respectively. In spite of the high activation barrier found for singlet TS1, it is predicted only 0.4 kcal/mol above the reactants asymptote, whereas the proton migration in triplet is achieved quite easily. An inversion in the relative stability of the singlet and triplet species is predicted in the step between the reactants

and the $Ti(OH)_2$ intermediate. Thus, the most stable triplet structure presents a linear geometry and $^3\Delta_g$ ground state, whereas singlet structure is predicted to have a $^1A_1$ state with planar $C_{2v}$ symmetry. The triplet and singlet species are calculated to be exothermic by about 27.0 and 10.3 kcal/mol regarding singlet reactants, respectively (see Figure 3). The spin crossing takes place in the vicinity of the singlet $Ti(OH)_2$ intermediate and a minimum energy crossing point, MECP1 (see Figure 5), has been characterized and localized by about 7.5 kcal/mol above the singlet structure of $Ti(OH)_2$. Subsequently, the formation of the product complex $O=Ti(H_2O)$ intermediate occurs by a proton migration from one OH group towards the adjacent OH group in the $Ti(OH)_2$ intermediate, via TS2. The activation barriers are predicted to be 36.3 and 34.7 kcal/mol on the triplet and singlet surfaces, respectively. However both transition states are localized above the reactants asymptote by 9.3 and 24.4 kcal/mol, being the most stable the triplet TS2 with an energy difference of 15.1 kcal/mol with respect to the singlet. Likewise, the triplet product complex $O=Ti(H_2O)$ is calculated to be 3.1 kcal/mol below the singlet reactants, whereas the singlet structure is found 8.0 kcal/mol higher than the triplet one. Finally, the water elimination is found to be an endothermic process of 16.5 kcal/mol. In this sense, Shao et al.[41] have studied the reaction of titanium oxides with water molecules, in particular the reaction: $^3TiO + H_2O \rightarrow {}^3Ti(OH)_2$. DFT calculations and experiments showed that the TiO is not able to react with $H_2O$ to led to $Ti(OH)_2$ intermediates indicating that the formation of the products $^3TiO + H_2O$ is not a reversible process.

On the other hand, the direct formation of the product complex $O=Ti(H_2O)$ from O=TiH(OH) takes place by means of Path2, via TS3. The singlet TS3 has an activation barrier of 55.1 kcal/mol and lies 15.7 kcal/mol above the reference, whereas triplet TS3 is predicted to be higher by about 42.1 kcal/mol. However, after singlet TS3 is reached,

a spin-crossing takes places in order to connect singlet and triplet PESs to yield the most stable triplet O=Ti($H_2O$) intermediate. Thus, a new minimum energy crossing point, MECP2 (see Figure 5), was localized in the vicinity of singlet TS3 by about 14.2 kcal/mol above the reactants asymptote.

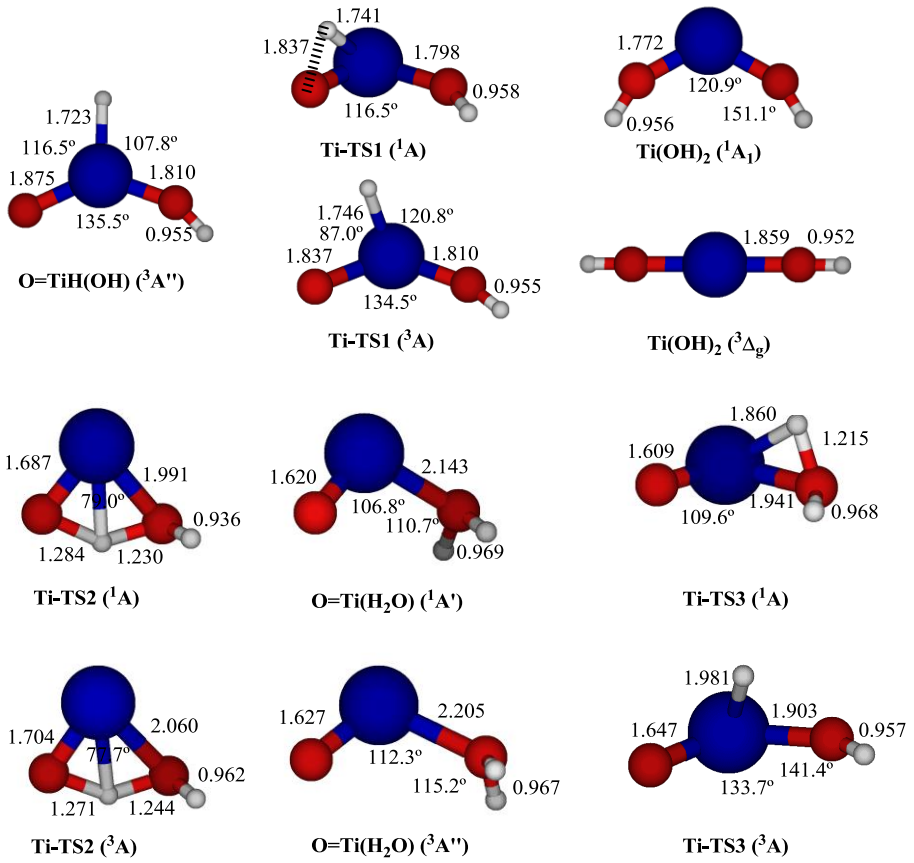


**Figure 4.** Optimized geometric parameters calculated at the B3LYP/6-311++G(2df,2pd)/SDD level of the involved species in the O=TiH(OH) → TiO + $H_2O$ step. Distances in angstroms and angles in degrees.

Finally, the reaction $TiO_2(^1A_1)$ + $H_2$ → TiO ($^3\Delta$) + $H_2O$ is predicted to be an endothermic process, 13.4 kcal/mol. The energy singlet TiO($^1\Delta$) is calculated to be 5.4 kcal/mol above the triplet ground state being underestimated regarding the experimental values of 9.85 ± 0.03 kcal/mol.[83]

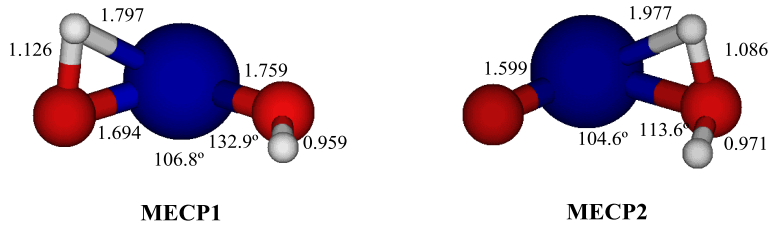


**Figure 5**. Structures of minimum energy crossing points, MECP1 and MECP2 found at the B3LYP/6-311++G(2df,2pd)/SDD for titanium oxide mechanisms. Distances in angstroms and angles in degrees.

**Zr.** From Path1, the singlet TS1 species present an activation barrier of 43.4 kcal/mol and it is calculated to be only 0.6 kcal/mol above the reactants. When the system reaches the stationary point of the $Zr(OH)_2$ structures an inverse order of stability is observed as previously seen along the titanium mechanism. Thus, our DFT calculations predict the triplet $Zr(OH)_2$ intermediate more stable in 5.5 kcal/mol (see Figure 3) than singlet one. These results are in good agreement with the CCSD(T)/cc-pVTZ-DK calculations reported by Syzgantseva et al. which predict the triplet $Zr(OH)_2$ more stable 6.0 kcal/mol than singlet one.[84] The $Zr(OH)_2$ molecules are calculated to have $C_2v$ symmetry, $^1A_1$ for singlet and and $^3B_1$ for triplet. A spin-crossing process takes place in the vicinity of the stationary point of the $Zr(OH)_2$ structures and a MECP3 has been localized. The MECP3 is calculated to be only 0.2 kcal/mol above singlet-$Zr(OH)_2$ while its structure is predicted to have a quasi-planar geometry with a OZrO angle of 118.2º, an intermediate value between the singlet and triplet $Zr(OH)_2$ species. In spite of MECP3 and singlet- $Zr(OH)_2$ were found very close in energy, both species present differences in their geometries (see Figure 6 and 7). Once the triplet $Zr(OH)_2$ intermediates is reached, the most stable transition state for TS2 is also found in triplet and its respective energy barrier is calculated to be 50.3 kcal/mol whereas the respective singlet TS2 is predicted to be only 3.3 kcal/mol higher than triplet one (see Figure 3). When the system reaches the stationary point of the $O=Zr(H_2O)$, triplet is still the most

stable electronic state. However, triplet O=Zr($H_2O$) lies only 0.3 kcal/mol below than the singlet and this gap is enhanced to 3.0 kcal/mol in separated products. On the contrary, the ground state of the ZrO molecule is experimentally found to be $^1\Sigma^+$ as mentioned above, therefore DFT calculations might be not able to predict the correct order of the relative energy. The reason for this is the DFT bias toward $4d^15s^1$ configurations over $4d^05s^2$.[27] This effect has been discussed by Bauschlicher and Langhoff,[85, 86] rendering that high levels of theory are required to describe correctly the electronic states of ZrO molecules due to the mixed bonding occurring among the $d^ns^2$, $d^{n+1}s^1$, $d^{n+2}$ Zr configurations.

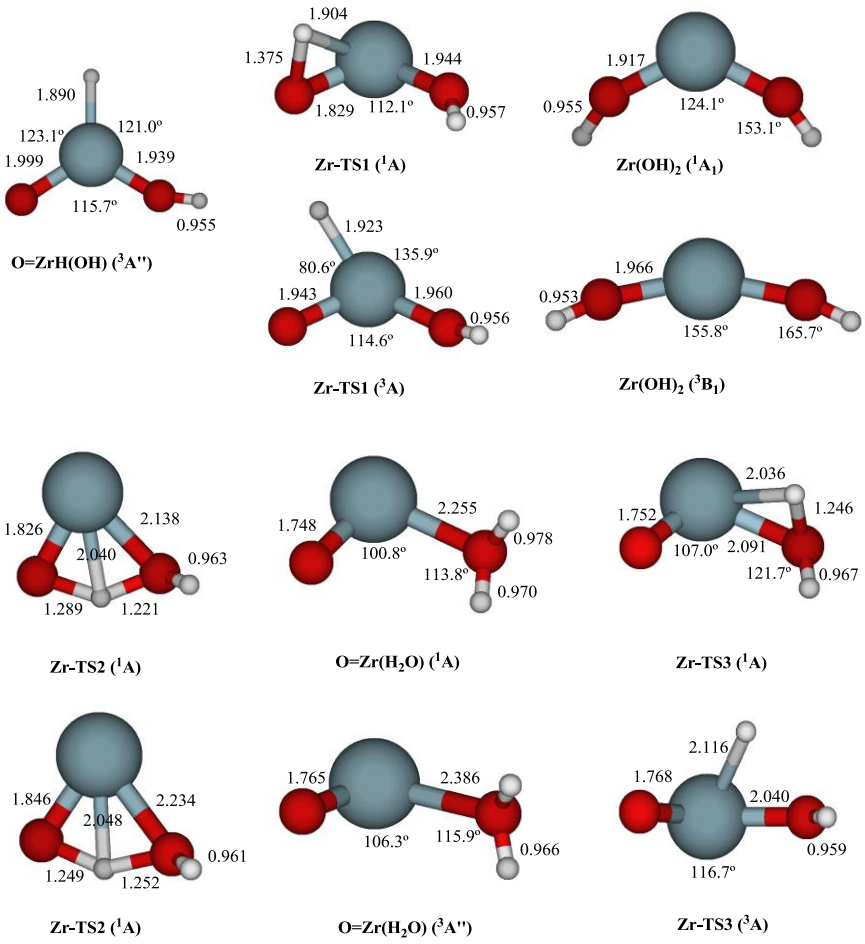


**Figure 6.** Optimized geometric parameters calculated at the B3LYP/6-311++G(2df,2pd)/SDD level of the involved species in the O=ZrH(OH) → ZrO + $H_2O$ step. Distances in angstroms and angles in degrees.

CASSCF/CASPT2 calculations revealed that both Path1 and Path2 seem to proceed through a single state reactivity (SSR) mechanism[65], namely, the reaction takes place only in singlet electronic state, although the singlet-triplet separation in some parts of the mechanism are too small to predict a conclusive answer. Singlet TS1, TS2, TS3, $Zr(OH)_2$ and $O=Zr(H_2O)$ were found more stable than their respective triplet species and therefore no spin-crossing process may be involved. While the singlet O=ZrH(OH) species is calculated to be 36.5 kcal/mol below the reactants asymptote, the singlet TS1 and TS2 were calculated with activation barriers of 43.7 and 45.2 kcal/mol, respectively, in good agreement with our previous DFT calculations. The singlet $Zr(OH)_2$ intermediate was computed more stable than the triplet, although at an energy almost degenerated with the triplet state (only 0.6 kcal/mol of difference; see Figure 3). The $O=Zr(H_2O)$ intermediate was predicted to be more stable in the singlet state, however the calculated CASSCF/CASPT2 singlet-triplet gap was 7.4 kcal/mol versus the 0.3 kcal/mol value predicted by the DFT method. In addition, the $^1\Sigma^+$-$^3\Delta$ separation of ZrO molecules was calculated to be 4.5 kcal/mol in excellent agreement with experimental value of 4.3 kcal/mol.[84]

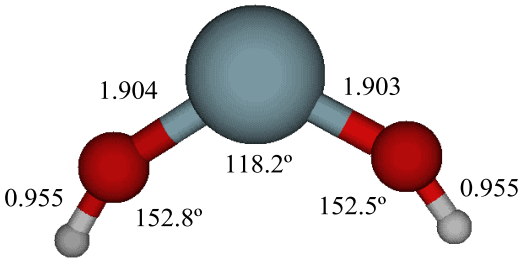


**MECP3**

**Figure 7.** Structure of minimum energy crossing point, MECP3 found at the B3LYP/6-311++G(2df,2pd)/SDD for zirconium oxide mechanisms. Distances in angstroms and angles in degrees.

Concerning Path2, the direct formation of the O=Zr($H_2O$) complex is achieved from O=ZrH(OH) intermediate via TS3. Both DFT and CASSCF/CASPT2 calculations have estimated an energy barrier of 59.2 kcal/mol in singlet electronic state. Finally the elimination of water complexes is calculated to be an endothermic process of 15.2 and 18.0 kcal/mol for DFT and CASSCF/CASPT2 calculations, respectively.

**Hf.** Concerning the reactivity of the $HfO_2$, as previously mentioned, the O=HfH(OH) is found to be the most stable of the hydride intermediates among the studied cases. Herein, the reactivity of the process takes place only in singlet electronic state since triplet was predicted to be considerably higher in energy in contrast to Ti and Zr mechanisms. Concerning Path1, the activation barrier associated with TS1 is calculated to be 36.6 kcal/mol and corresponds to the lowest activation barrier in comparison with Ti and Zr mechanisms. Additionally, TS1 is calculated to be 17.7 kcal/mol below the reactants asymptote and therefore the formation of the intermediate $Hf(OH)_2$ should be expected to be a spontaneous process. Likewise, $Hf(OH)_2$ is found 1.3 kcal/mol above the O=Hf(OH) intermediate with $C_2v$ symmetry. The proton migration process between both OH groups, via TS2, leads to the water complex with an energy barrier of 52.8 kcal/mol. Despite the high value of the activation barrier, TS2 only lies 0.1 kcal/mol above the reactants asymptote. In contrast, the water complex is obtained with $C_1$ symmetry and is calculated to be 11.5 kcal/mol below the reactants, nevertheless the $C_s$ water complex presents an imaginary frequency value associated with the rotation of water and therefore is not considered in the reactive process. On the other hand, concerning Path2 the direct formation of the O=Hf($H_2O$) complex from the hydride intermediate takes place via TS3 which has associated an energy barrier of 56.0 kcal/mol. This barrier is calculated to be 1.9 kcal/mol higher than the barrier associated

with TS2. Finally, the water complex formed can dissociate easily to final products due to overall exothermicity of the reaction. Thus, the water elimination step is calculated to be 10.5 kcal/mol and the whole process is found to be an exothermic process of $\Delta E$= -1.0 kcal/mol.

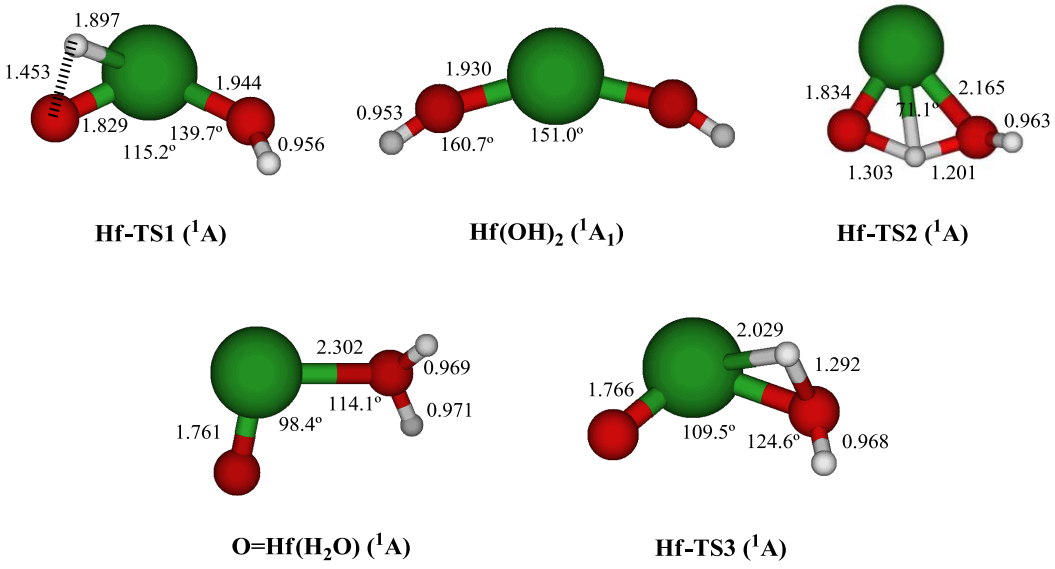


**Figure 8** Optimized geometric parameters calculated at the B3LYP/6-311++G(2df,2pd)/SDD level of the species involved in the O=HfH(OH) → HfO + $H_2O$ step. Distances in angstroms and angles in degrees.

## 4. Discussion Concerning the Differences among $MO_2$ reaction mechanisms

The global view of the hydrogenation process shows that the dihydrogen cleavage step is feasible in all $MO_2$ cases yielding to large exothermic O=MH(OH) intermediates. Nevertheless, the reactivity of the processes along the explored reaction pathways was found to have a strong dependence of the metal centre. Thus, while $TiO_2$ dioxide presents significant differences of geometry and vibrational frequencies in comparison to $ZrO_2$ and $HfO_2$ (see Table 1), both $ZrO_2$ and $HfO_2$ display very similar molecular geometries in conjunction with the lack of a measurable difference in their vibrational frequencies. This similarity is commonly attributed to the lanthanide contraction of Hf that is responsible for the similar atomic and ionic radii of Zr and Hf as well as their

similar ionization potentials. However, important differences are found their respective electroaffinity.[7] In particular the electron affinities of $TiO_2$ and $ZrO_2$ dioxides are rather similar, whereas the electron affinities of $HfO_2$ and $ZrO_2$ differ substantially[7]. This fact demonstrates the nonnegligible role of f-electrons and relativistic effects in the chemistry of hafnium compounds. Therefore, it seems to indicate electronic structure rather than size or bonding effects as the primary basis for reactivity differences among $TiO_2$, $ZrO_2$ and $HfO_2$ mechanisms.[7]

While the parallelism between structural properties of bulk phases and molecular systems is limited, it is possible to correlate a number of properties. For example it is well known that for both molecular systems and bulks materials $TiO_2$, $ZrO_2$ and $HfO_2$ are highly polar.[7, 75] Thus, the experimental measure of dipole moments[69, 87] of $TiO_2$, $ZrO_2$ and $HfO_2$, 6.7 of 7.80 and 7.92 *D*, respectively, confirms the difference in ionicity. The availability of *n*s and (*n*-1)d orbitals on the metal atom, discarding the *n*p orbitals which are higher in energy, makes the charge distribution of an excess electron different than in anions of polar molecules that do not contain a transition metal atom. Hence, an excess electron bound by a polar molecule is described by a fully symmetric sd-type hybrid orbital with $a_1$ symmetry and therefore it might explain the large stability of the O=MH(OH) intermediates as well as the decreasing of the energy barrier associated with the dihydrogen cleavage as the metal center increases. Therefore it is expected that as the metal center size increases the respective hydride O=MH(OH) species should be less reactive for catalytic processes.

On the other hand, when the reaction mechanisms are compared some important differences arise. For example, the difference in energy between singlet TS1 and TS3 of 15.3 kcal/mol clearly favors Path1 instead of Path2 for $TiO_2$ mechanisms, and therefore the process may take place through $Ti(OH)_2$ intermediates. In contrast, no experimental

evidence has been found for the reaction of hydrolysis of titanium monoxide, $^3$TiO + $H_2O$, yielding to $Ti(OH)_2$ intermediate[41] indicating that the reaction is not reversible. Thus, the whole reaction mechanism proceeds in three steps by means of a spin crossing singlet-triplet process where MECP1 is localized in the vicinity of $Ti(OH)_2$ intermediates.

In the case of $ZrO_2$ mechanisms the process is also controlled by the reactivity of Path1. The direct formation of O=Zr($H_2O$) from O=ZrH(OH) requires a higher activation energy of 59.2 kcal/mol versus 43.7 kcal/mol of TS1 in Path1. Likewise, spin-crossing effects have been discarded since CASSCF/CASPT2 calculations displays that the process takes place only in singlet electronic state. However, DFT calculations are in good agreement with multiconfigurational methods with the exception of the relative stability order of $Zr(OH)_2$, O=Zr($H_2O$) and ZrO species.

The dihydrogen activation by $HfO_2$ is predicted to be the most favorable process with the lowest activation barrier and the largest exothermicity of its hydride intermediate O=HfH(OH), being the most plausible mechanism Path 1 as previously found for both $TiO_2$ and $ZrO_2$ systems. Likewise O=HfH(OH) and $Hf(OH)_2$ intermediates were found quite close in energy, but the strong stability of these species makes the $HfO_2$ reactivity less interesting for catalytic proposes.

In addition, spin-crossings might not be expected on systems involving zirconium nor hafnium because of the spin-orbit coupling is large for heavy atoms. TSR is expected for 3d transition metals, and perhaps also for the 4d block. For 4f, 5d, and 5f elements, the maximum probability of spin inversion (*p*SI) is assumed , i.e *p*SI = 1, and therefore the spin-crossings are completely avoided.[65] All the quantum-chemical calculations predict Path 1 as the most feasible reaction pathway; for titanium it is clearly favored.

The results obtained in the present paper for $MO_2$ molecules are consistent with the observed reactivity on surfaces. Rutile $TiO_2$ (110) monocrystal is known to be inactive towards $H_2$ dissociation, and no Ti-H groups are found to be stabilized.[88] However, the hydrogenated surfaces exist but they originate from the dissociation of water on oxygen vacancies.[16] Monoclinic $ZrO_2$ surfaces dissociate more easily $H_2$ (barriers around 8 kcal/mol) and Zr-H groups are stable and detected by IR spectroscopy.[89] For $HfO_2$ no data have been found in the literature concerning hydrogenation mechanisms, and we predict the easy dissociation of dihydrogen, and the stability of Hf-H groups.

## 5. Conclusions

We have presented a detailed computational study on the key steps for the reaction mechanism of $H_2$ oxidation by $MO_2$ molecules: $MO_2 + H_2 \rightarrow MO + H_2O$ (M = Ti, Zr, and Hf). Optimized geometrical parameters and vibrational analysis of $MO_2$ and MO molecules agree with experimental data allowing to validate the B3LYP/6-311++G(2df,2pd)/SDD methodology employed in the present study. Important mechanistic insights can be obtained from the calculation of geometries and energies of the species involved along the corresponding reaction pathways. The hydrogen activation by means of $MO_2$ molecules has a strong dependence of metal center indicating that the electronic structure rather than size or bonding effects are the primary basis for reactivity differences among $TiO_2$, $ZrO_2$ and $HfO_2$ mechanisms. Thus, the results show that the exothermicity of the O=MH(OH) species increases in reverse order as the activation barriers of the dihydrogen cleavage.

The formation of products $MO + H_2O$ is predicted to be favorable through Path1 in all the studied cases and therefore the presence of $M(OH)_2$ species along the reaction pathway is expected. In particular, only titanium reaction pathways take place by means

of TSR mechanism. While Hf dioxide is expected to be the most favorable process because of its exothermicity, however the high stability of the O=HfH(OH) and $Hf(OH)_2$ makes the reactivity of $HfO_2$ less interesting for catalytic purposes.

## 6. Acknowledgments

Financial support from *Ministerio de Ciencia e Innovación* (MICINN) for projects CTQ2009-14541-C02 and CTQ2010-14892, and Generalitat Valenciana for *Prometeo*/2009/053 project is gratefully acknowledged. The authors are also grateful to the Servei d'Informatica, Universitat Jaume I, DSI-CCRE and GENCI-IDRIS (grants x2010082131, x2011082131 and x2012082131) for computational facilities. P.G-N would like to thank to the HPC-EUROPA2 project (project number: 228398) for the support of the European Commission - Capacities Area - Research Infrastructures. F. R. would like to thank the Eusko Jaurlaritza (GIC 07/85 IT-330-07) for financial support and the Spanish Office for Scientific Research (CTQ2011-27374). The SGI/IZO-SGIker UPV/EHU is gratefully acknowledged for generous allocation of computational resources.

7. **Supporting Information Available:** Additional information concerning complete references 52 and 61 are available. This material is available free of charge via the Internet at http://pubs.acs.org.

## 8. References


(1) Bell, A. T. The Impact of Nanoscience on Heterogeneous Catalysis. *Science* **2003**, *299*, 1688-1691.

(2) Li, M. H.; Shen, J. Y. Microcalorimetric Adsorption Characterizations of Supported Vanadia Catalysts for the Selective Oxidation of Propylene to Acetone. *J. Cat.* **2002**, *205*, 248-258.

(3) Martinez-Huerta, M. V.; Gao, X.; Tian, H.; Wachs, I. E.; Fierro, J. L. G.; Banares, M. A. Oxidative Dehydrogenation of Ethane to Ethylene over Alumina-Supported Vanadium Oxide Catalysts: Relationship between Molecular Structures and Chemical Reactivity. *Catal. Today* **2006**, *118*, 279-287.

(4) Zhao, C. L.; Wachs, I. E. Selective Oxidation of Propylene to Acrolein over Supported $V_2O_5/Nb_2O_5$ catalysts: An in Situ Raman, IR, TPSR and Kinetic Study. *Catal. Today* **2006**, *118*, 332-343.

(5) Centi, G.; Cavani, F.; Trifiro, F., *Selective Oxidation by Heterogeneous Catalysis*; Kluwer Academic: Plenum Publishers, New York, 2001.

(6) Thomas, J. M.; Thomas, W. J., *Principles and Practice of Heterogeneous Catalysis*; VCH: Weinheim, New York, 1997.

(7) Zheng, W. J.; Bowen, K. H.; Li, J.; Dabkowska, I.; Gutowski, M. Electronic Structure Differences in $ZrO_2$ vs $HfO_2$. *J. Phys. Chem. A* **2005,** *109*, 11521-11525.

(8) Kubas, G. J. Fundamentals of $H_2$ Binding and Reactivity on Transition Metals Underlying Hydrogenase Function and $H_2$ Production and Storage. *Chem. Rev.* **2007,** *107*, 4152-4205.

(9) Nishimura, S., *Handbook of Heterogeneous Catalytic Hydrogenation for Organic Synthesis*; J. Wiley, New York, 2001.

(10) Vries, J. G. d.; Elsevier, C. J., *The Handbook of Homogeneous Hydrogenation*; Wiley-VCH: Weinheim, Great Britain, 2007.

(11) Berke, H. Conceptual Approach to the Reactivity of Dihydrogen. *Chemphyschem* **2010**, *11*, 1837-1849.

(12) Bohme, D. K.; Schwarz, H. Gas-phase Catalysis by Atomic and Cluster Metal Ions: The Ultimate Single-Site Catalysts. *Angew. Chem. Int. Edit.* **2005**, *44*, 2336-2354.

(13) Zhao, Y.-X.; Wu, X.-N.; Ma, J.-B.; He, S.-G.; Ding, X.-L. Characterization and Reactivity of Oxygen-Centred Radicals over Transition Metal Oxide Clusters. *Phys. Chem. Chem. Phys.* **2011**, *13*, 1925-1938.

(14) Henrich, V. E.; Cox, P. A., *The Surface Science of Metal Oxides*; Cambridge University Press: Cambridge, New York, 1994.

(15) Wu, H.; Wang, L. Electronic Structure of Titanium Oxide: $TiO_y$ (y=1-3). *J. Chem. Phys.* **1997**, *107*, 8221.

(16) Diebold, U. The Surface Science of Titanium Dioxide. *Surf. Sci. Rep.* **2003**, *48*, 53-229.

(17) Gratzel, M. Photoelectrochemical Cells. *Nature* **2001**, *414*, 338-344.

(18) Fujishima, A.; Honda, K. Electrochemical Photolysis of Water at a Semiconductor Electrode. *Nature* **1972**, *238*, 37.

(19) Yahaya, A. H.; Gondal, M. A.; Hameed, A. Selective Laser Enhanced Photocatalytic Conversion Of $CO_2$ into Methanol. *Chem. Phys. Lett.* **2004**, *400*, 206-212.

(20) Salem, I. Recent Studies on the Catalytic Activity of Titanium, Zirconium, and Hafnium Oxides. *Cat. Rev. Sci. Eng.***2003**, *45*, 205-296.

(21) Reddy, B. M.; Khan, A. Recent Advances on $TiO_2$-$ZrO_2$ Mixed Oxides as Catalysts and Catalyst Supports. *Cat. Rev. Sci. Eng.***2005**, *47*, 257-296.

(22) Nahar, R. K.; Singh, V.; Sharma, A. Study of Electrical and Microstructure Properties of High Dielectric Hafnium Oxide Thin Film for MOS Devices. *J. Mater. Sci. Mater. Electron.***2007**, *18*, 615-619.
(23) Dixit, S. K.; Zhou, X. J.; Schrimpf, R. D.; Fleetwood, D. M.; Pantelide, S. T.; Choi, R.; Bersuker, G.; Feldman, L. C. Radiation Induced Charge Trapping in Ultrathin $HfO_2$-Based MOSFETs. *Ieee T. Nucl. Sci.* **2007**, *54*, 1883-1890.
(24) Chiodo, S.; Kondakova, O.; Michelini, M. D.; Russo, N.; Sicilia, E.; Irigoras, A.; Ugalde, J. M. Theoretical Study of Two-State Reactivity of Transition Metal Cations: The "Difficult" Case of Iron Ion Interacting With Water, Ammonia, And Methane. *J. Phys. Chem. A* **2004**, *108*, 1069-1081.
(25) Matxain, J. M.; Mercero, J. M.; Irigoras, A.; Ugalde, J. M. Discordant Results on the $FeO^+ + H_2$ Reaction Reconciled by Quantum Monte Carlo Theory. *Mol. Phys.* **2004**, *102*, 2635-2637.
(26) Irigoras, A.; Fowler, J. E.; Ugalde, J. M. Reactivity of Cr+(S-6,D-4), Mn+(S-7,S-5), and Fe+(D-6,F-4): Reaction of Cr+, Mn+, and Fe+ with Water. *J. Am. Chem. Soc.* **1999**, *121*, 8549-8558.
(27) Filatov, M.; Shaik, S. Theoretical Investigation of Two-State-Reactivity Pathways of H-H Activation by FeO+: Addition-Elimination, "Rebound", and Oxene-Insertion Mechanisms. *J. Phys. Chem. A* **1998**, *102*, 3835-3846.
(28) Irigoras, A.; Fowler, J. E.; Ugalde, J. M. On the Reactivity of Ti+(F-4,F-2). Reaction of Ti+ with $OH_2$. *J. Phys. Chem. A* **1998**, *102*, 293-300.
(29) Schroder, D.; Schwarz, H.; Clemmer, D. E.; Chen, Y. M.; Armentrout, P. B.; Baranov, V. I.; Bohme, D. K. Activation of Hydrogen and Methane by Thermalized FeO+ in the Gas Phase as Studied by Multiple Mass Spectrometric Techniques. *Int. J. Mass Spectrom. Ion Processes* **1997**, *161*, 175-191.
(30) Fiedler, A.; Kretzschmar, I.; Schroder, D.; Schwarz, H. Chromium Dioxide Cation OCrO+ in the Gas Phase: Structure, Electronic States, and the Reactivity with Hydrogen and Hydrocarbons. *J. Am. Chem. Soc.* **1996**, *118*, 9941-9952.
(31) Heinemann, C.; Cornehl, H. H.; Schroder, D.; Dolg, M.; Schwarz, H. The $CeO_2^+$ Cation: Gas-phase Reactivity and Electronic Structure. *Inorg. Chem.* **1996**, *35*, 2463-2475.
(32) Irigoras, A.; Ugalde, J. M.; Lopez, X.; Sarasola, C. On the Dissociation Energy of $Ti(OH_2)+$. An MCSCF, CCSD(T), and DFT study. *Can. J. Chem.* **1996**, *74*, 1824-1829.
(33) Ryan, M. F.; Fiedler, A.; Schroder, D.; Schwarz, H. Radical-like Behavior of Manganese Oxide Cation in its Gas-Phase Reactions with Dihydrogen and Alkanes. *J. Am. Chem. Soc.* **1995**, *117*, 2033-2040.
(34) Ryan, M. F.; Fiedler, A.; Schroder, D.; Schwarz, H. Stoichiometric Gas-Phase Oxidation Reactions of COO+ with Molecular Hydrogen, Methane, and Small Alkanes. *Organometallics* **1994**, *13*, 4072-4081.
(35) Schroder, D.; Fiedler, A.; Ryan, M. F.; Schwarz, H. Surprisingly Low Reactivity of Bare FeO+ in its Spin-Allowed, Highly Exothermic Reaction with Molecular Hydrogen to Generate Fe+ and Water. *J. Phys. Chem.* **1994**, *98*, 68-70.
(36) Kappes, M. M.; Staley, R. H. Oxidation of Transition-Metal Cations in the Gas-Phase - Oxygen Bond-Dissociation Energies and Formation of an Excited-State Product. *J. Phys. Chem.* **1981**, *85*, 942-944.
(37) Kappes, M. M.; Staley, R. H. Gas-Phase Oxidation Catalysis by Transition-Metal Cations. *J. Am. Chem. Soc.* **1981**, *103*, 1286-1287.

(38) Zhou, M. F.; Wang, C. X.; Li, Z. H.; Zhuang, J.; Zhao, Y. Y.; Zheng, X. M.; Fan, K. N. A. Spontaneous Dihydrogen Activation by Neutral $TaO_4$ Complex at Cryogenic Temperatures. *Angew. Chem. Int. Edit.* **2010**, *49*, 7757-7761.
(39) Hwang, D. Y.; Mebel, A. M. Ab Initio Study of the Reaction Mechanisms of NiO and NiS with $H_2$. *J. Phys. Chem. A* **2002**, *106*, 520-528.
(40) Zhou, M.; Zhang, L.; Lu, H.; Shao, L.; Chen, M. Reaction of Silicon Dioxide with Water: a Matrix Isolation Infrared and Density Functional Theoretical Study. *J. Mol. Struc.* **2002**, *605*, 249-254.
(41) Shao, L. M.; Zhang, L. N.; Chen, M. H.; Lu, H.; Zhou, M. F. Reactions of Titanium Oxides with Water Molecules. A Matrix Isolation FTIR and Density Functional Study. *Chem. Phys. Lett.* **2001**, *343*, 178-184.
(42) Zhang, L. N.; Shao, L. M.; Zhou, M. F. Reactions of Laser-Ablated Y and La Atoms with $H_2O$ Infrared Spectra and Density Functional Calculations of the HMO, HMOH and $M(OH)_2$ Molecules in Solid Argon. *Chem. Phys.* **2001**, *272*, 27-36.
(43) Zhang, L. N.; Zhou, M. F.; Shao, L. M.; Wang, W. N.; Fan, K. N.; Qin, Q. Z. Reactions of Fe with $H_2O$ and FeO with $H_2$. A Combined Matrix Isolation FTIR and Theoretical Study. *J. Phys. Chem. A* **2001**, *105*, 6998-7003.
(44) Zhou, M. F.; Zhang, L. N.; Shao, L. M.; Wang, W. N.; Fan, K. N.; Qin, Q. Z. Reactions of Mn with $H_2O$ and MnO with $H_2$. Matrix-isolation FTIR and Quantum Chemical Studies. *J. Phys. Chem. A* **2001**, *105*, 5801-5807.
(45) Rollason, R. J.; Plane, J. M. C. The reactions of FeO with $O_3$, $H_2$, $H_2O$, $O_2$ and $CO_2$. *Phys. Chem. Chem. Phys.* **2000**, *2*, 2335-2343.
(46) Calatayud, M.; Maldonado, L.; Minot, C. Reactivity of $(TiO_2)_N$ clusters (N = 1-10): Probing Gas-Phase Acidity and Basicity Properties. *J. Phys. Chem. C* **2008**, *112*, 16087-16095.
(47) Calatayud, M.; Minot, C. Is There a Nanosize for the Activity of $TiO_2$ Compounds? *J. Phys. Chem. C* **2009**, *113*, 12186-12194.
(48) Li, S.; Dixon, D. A. Molecular Structures and Energetics of the $(TiO_2)_n$ (n = 1-4) Clusters and their Anions. *J. Phys. Chem. A* **2008**, *112*, 6646-6666.
(49) Matsuda, Y.; Bernstein, E. R. On the Titanium Oxide Neutral Cluster Distribution in the Gas Phase: Detection through 118 nm Single-Photon and 193 nm Multiphoton Ionization. *J. Phys. Chem. A* **2005**, *109*, 314-319.
(50) Qu, Z.-w.; Kroes, G.-J. Theoretical Study of the Electronic Structure and Stability of Titanium Dioxide Clusters $(TiO_2)_n$ with n = 1-9. *J. Phys. Chem. B* **2006**, *110*, 8998-9007.
(51) Zhou, M.; Wang, C.; Zhuang, J.; Zhao, Y.; Zheng, X. Matrix Isolation Spectroscopic and Theoretical Study of Dihydrogen Activation by Group V Metal Dioxide Molecules. *J. Phys. Chem. A* **2011**, *115*, 39-46.
(52) Gaussian 03; Revision D.02; Frisch, M. J.; Trucks, G. W.; Schlegel, H. B.; Scuseria, G. E.; Robb, M. A.; Cheeseman, J. R.; Montgomery, Jr., J. A.; Vreven, T.; Kudin, K. N.; Burant, J. C.; et. al., Gaussian, Inc., Wallingford CT, 2004.
(53) Becke, A. D. Density-Functional Exchange-Energy Approximation with correct Asymptotic-Behavior. *Phys. Rev. A* **1988**, *38*, 3098-3100.
(54) Becke, A. D. A New Mixing of Hartree-Fock and Local Density-Functional Theories. *J. Chem. Phys.* **1993**, *98*, 5648.
(55) Fukui, K. Formulation of the Reaction Coordinate. *J. Phys. Chem.* **1970**, *74*, 4161-4163.
(56) Andrae, D.; Haussermann, U.; Dolg, M.; Stoll, H.; Preuss, H. Energy-Adjusted Abinitio Pseudopotentials for the 2nd and 3rd Row Transition-Elements. *Theor. Chim. Acta* **1990**, *77*, 123-141.

(57) Andersson, K.; Malmqvist, P. A.; Roos, B. O. 2nd-order Perturbation-Theory with a Complete Active Space Self-Consistent Field Reference Function. *J. Chem. Phys.* **1992**, *96*, 1218-1226.
(58) Roos, B. O.; Lindh, R.; Malmqvist, P. A.; Veryazov, V.; Widmark, P. O. New Relativistic ANO Basis Sets for Transition Metal Atoms. *J. Phys. Chem. A* **2005**, *109*, 6575-6579.
(59) Ghigo, G.; Roos, B. O.; Malmqvist, P. A. A Modified Definition of the Zeroth-Order Hamiltonian in Multiconfigurational Perturbation Theory (CASPT2). *Chem. Phys. Lett.* **2004**, *396*, 142-149.
(60) Forsberg, N.; Malmqvist, P. A. Multiconfiguration Perturbation Theory with Imaginary Level Shift. *Chem. Phys. Lett.* **1997**, *274*, 196-204.
(61) Aquilante, F.; De Vico, L.; Ferre, N.; Ghigo, G.; Malmqvist, P.-A.; Neogrady, P.; Pedersen, T. B.; Pitonak, M.; Reiher, M.; Roos, B. O.; et al. Software News and Update MOLCAS 7: The Next Generation. *J. Comput. Chem.* **2010**, *31*, 224-247.
(62) Armentrout, P. B. Chemistry of Excited Electronic States. *Science* **1991**, *251*, 175-179.
(63) Rue, C.; Armentrout, P. B.; Kretzschmar, I.; Schroder, D.; Harvey, J. N.; Schwarz, H. Kinetic-Energy Dependence of Competitive Spin-Allowed and Spin-Forbidden Reactions: $V^+ + CS_2$. *J. Chem. Phys.* **1999**, *110*, 7858-7870.
(64) Shaik, S.; Hirao, H.; Kumar, D. Reactivity of High-Valent Iron-Oxo Species in Enzymes and Synthetic Reagents: A Tale of Many States. *Acc. Chem. Res.***2007**, *40*, 532-542.
(65) Schroder, D.; Shaik, S.; Schwarz, H. Two-State Reactivity as a New Concept in Organometallic Chemistry. *Acc. Chem. Res.***2000**, *33*, 139-145.
(66) Gracia, L.; Sambrano, J. R.; Safont, V. S.; Calatayud, M.; Beltran, A.; Andres, J. Theoretical Study on the Molecular Mechanism for the Reaction of $VO_2^+$ with $C_2H_4$. *J. Phys. Chem. A* **2003**, *107*, 3107-3120.
(67) Harvey, J. N.; Aschi, M.; Schwarz, H.; Koch, W. The Singlet and Triplet States of Phenyl Cation. A Hybrid Approach for Locating Minimum Energy Crossing Points between Non-Interacting Potential Energy Surfaces. *Theor. Chem. Acc.* **1998**, *99*, 95-99.
(68) Chertihin, G. V.; Andrews, L. Reactions of Laser-Ablated Titanium, Zirconium, and Hafnium Atoms with Oxygen Molecules in Condensing Argon. *J. Phys. Chem.* **1995**, *99*, 6356-6366.
(69) Lesarri, A.; Suenram, R. D.; Brugh, D. Rotational Spectrum of Jet-Cooled $HfO_2$ and HfO. *J. Chem. Phys.* **2002**, *117*, 9651-9662.
(70) Brugh, D. J.; Suenram, R. D.; Stevens, W. J. Fourier Transform Microwave Spectroscopy of Jet-Cooled $ZrO_2$ Produced by Laser Vaporization. *J. Chem. Phys.* **1999,** *111*, 3526-3535.
(71) Amiot, C.; Luc, P.; Vetter, R. Isotope Shifts in the TiO B-X (1-0) band. *J. Mol. Spectrosc.* **2002**, *214*, 196-201.
(72) Huber, K.-P.; Herzberg, G., *Constants of Diatomic Molecules*. Van Nostrand Reinhold: New York, 1979.
(73) Ram, R. S.; Bernath, P. F.; Dulick, M.; Wallace, L. The A(3)Phi-X-3 Delta System (Gamma Bands) of TiO: Laboratory and Sunspot Measurements. *Astrophys. J. Suppl. S.* **1999**, *122*, 331-353.
(74) Grein, F. Density Functional Theory and Multireference Configuration Interaction Studies on Low-Lying Excited States of $TiO_2$. *J. Chem. Phys.* **2007**, *126*, 034313
(75) Li, S. G.; Dixon, D. A. Molecular Structures and Energetics of the $(ZrO_2)_n$ and $(HfO_2)_n$ (n=1-4) Clusters and their Anions. *J. Phys. Chem. A* **2010**, *114*, 2665-2683.

(76) Miliordos, E.; Mavridis, A. Electronic Structure and Bonding of the Early 3d-Transition Metal Diatomic Oxides and Their Ions: $ScO^{0,+/-}$, $TiO^{0,+/-}$, $CrO^{0,+/-}$, and $MnO^{0,+}$. *J. Phys. Chem. A* **2010**, *114*, 8536-8572.
(77) Mok, D. K. W.; Lee, E. P. F.; Chau, F. T.; Dyke, J. M. A Combined Ab Initio and Franck-Condon Factor Simulation Study on the Photodetachment Spectrum of $HfO_2$. *Phys. Chem. Chem. Phys.* **2008**, *10*, 7270-7277.
(78) Spohn, B.; Goll, E.; Stoll, H.; Figgen, D.; Peterson, K. A. Energy-Consistent Pseudopotentials for the 5d Elements-Benchmark Calculations for Oxides, Nitrides, and Pt(2). *J. Phys. Chem. A* **2009**, *113*, 12478-12484.
(79) Todorova, T. K.; Infante, I.; Gagliardi, L.; Dyke, J. M. The Chemiionization Reactions Ce + O and Ce + $O_2$: Assignment of the Observed Chemielectron Bands. *Int. J. Quantum Chem.* **2009**, *109*, 2068-2079.
(80) Wang, S. G.; Schwarz, W. H. E. Lanthanide Diatomics and Lanthanide Contractions. *J. Phys. Chem.* **1995**, *99*, 11687-11695.
(81) Wu, Z. J.; Guan, W.; Meng, J.; Su, Z. M. Density Functional Studies of Diatomic LaO to LuO. *J. Clust. Sci.* **2007**, *18*, 444-458.
(82) Zhao, Y. X.; Ding, X. L.; Ma, Y. P.; Wang, Z. C.; He, S. G. Transition Metal Oxide Clusters with Character of Oxygen-Centered Radical: a DFT study. *Theor. Chem. Acc.* **2010**, *127*, 449-465.
(83) Amiot, C.; Cheikh, M.; Luc, P.; Vetter, R. The TiO c(1)Phi-a(1)Delta (0-0) Band at Sub-Doppler Spectral Resolution: Spin-Orbit Interactions in the c state. *J. Mol. Spectrosc.* **1996**, *179*, 159-167.
(84) Syzgantseva, O.; Calatayud, M.; Minot, C. Theoretical Study of $H_2$ Dissociation on a $ZrO_2$ Cluster. *Chem. Phys. Lett.* **2011**, *503*, 12-17.
(85) Bauschlicher, C. W.; Langhoff, S. R. The Study of Molecular Spectroscopy by Ab Initio Methods. *Chem. Rev.* **1991**, *91*, 701-718.
(86) Langhoff, S. R.; Bauschlicher, C. W. Theoretical-Study of the Spectroscopy of ZrO. *Astrophys. J.* **1990**, *349*, 369-375.
(87) Bruenken, S.; Mueller, H. S. P.; Menten, K. M.; McCarthy, M. C.; Thaddeus, P. The Rotational Spectrum of $TiO_2$. *Astrophys. J.* **2008**, *676*, 1367-1371.
(88) Yin, X. L.; Calatayud, M.; Qiu, H.; Wang, Y.; Birkner, A.; Minot, C.; Woell, C. Diffusion versus Desorption: Complex Behavior of H Atoms on an Oxide Surface. *Chemphyschem* **2008**, *9*, 253-256.
(89) Syzgantseva, O.; Calatayud, M.; Minot, C. Hydrogen Adsorption on Monoclinic (111) and (101) $ZrO_2$ surfaces: A Periodic Ab Initio Study. *J. Phys. Chem. C* **2010**, *114*, 11918-11923.

# TOC Graphic

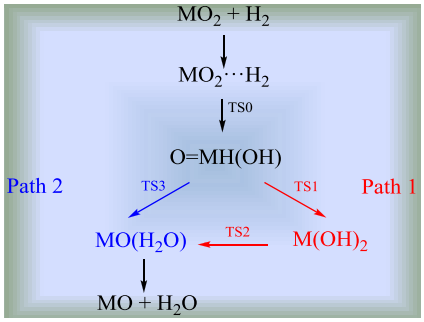
MO2 + H2
MO2···H2
TS0
O=MH(OH)
Path 2
TS3
TS1
Path 1
MO(H2O)
TS2
M(OH)2
MO + H2O